CrystEngComm

Accepted Manuscript

ROYAL SOCIETY OF CHEMISTRY

www.rsc.org/crystengcomm

Structures of the Conformational Isomers and Polymorph Modifications of N-substituted 2,6-(E,E)-bis(ferrocenylidene)piperid-4-ones. Photo- and electrochemically induced E/Z isomerization

Alexander S. Romanov,[‡,⊥] Gary F. Angles,[⊥] Alexey V. Shapovalov,[‡] Fabrizia F. Fabrizi de Biani,[§] Maddalena Corsini,[§] Stefania Fusi,[§] Tatiana V. Timofeeva[⊥,*]

[‡]Institute of Organoelement Compounds, Russian Academy of Sciences, 119991 Moscow, Russian Federation, [⊥]Department of Natural Sciences, New Mexico Highlands University, Las Vegas, New Mexico 87701, [§] Dipartimento di Biotecnologie Chimica e Farmacia Università di Siena, 53100 Siena, Italy

Abstract

Four N-substituted 2,6-(E,E)-bis(ferrocenylidene)piperid-4-ones (NH **1**, NMe **2**, NEt **3**, NCH_2Ph **4**) were prepared by aldol condensation between ferrocenecarbaldehyde and two equivalents of N-substituted piperid-4-ones with high yields. The N-protonated compounds were obtained by reaction with $HBF_4 \cdot Et_2O$ acid. The molecular structure of compounds **2**, **3**, **2**·HBF_4 and **4**·HBF_4 were confirmed with X-ray diffraction analysis and three types of the conformational isomers were elucidated. Two polymorph modifications were found for compound **2**·HBF_4. The electron transfer properties of the complexes were examined by electrochemical and spectroelectrochemical techniques. The complexes **1**–**4** undergo a reversible processes of two-electron oxidation and partially reversible one-electron reduction. Photo- and electrochemically induced E/Z isomerisation of complexes was monitored with UV-vis and ^1H NMR spectra.

Keywords: Ferrocene; Polymorph; Crystal Structure; Spectroelectrochemistry; Aldol Condensation.

Introduction

For decades a variety of cross-conjugated bis(arylideneacetone) derivatives (Ar–CH=CH–C(O)–CH=CH–Ar, where Ar = arene) attracted significant attention due to several reasons: straightforward synthetic procedures (one-step reaction – aldol condensation),[1] a number of useful properties for medicinal chemistry and materials science. For instance, such compounds are considered as synthetic analogues of curcumin (1,7-bis(4-hydroxy-3-methoxyphenyl)1,6-heptadien-3,5-dion), which is a natural component of the rhizome of *Curcuma longa*,[2] containing conjugated diene system as a pharmacophore fragment. In this view, 3,5-bis(arylidene)piperid-4-ones are considered as prospective compounds with cytotoxic,[3] antitumor,[4,5] anticancer, [5] antioxidant,[6] and antimycobacterial properties,[7] or antineoplasmatic agents,[8] which prone to selective accumulation neoplastic formations and presents significantly higher bioactivity than curcumin.

One of intrinsic potential application of 3,5-bis(arylidene)piperid-4-ones is their use as the two-photon photodynamic sensitizers for photodynamic therapy of cancer due to their Donor-π-Acceptor-π-Donor structure. A number of materials both porphyrin-[9] and non-porphyrin-[10] based were reported to as two-photon sensitizers but significant drawbacks when compared to arylidenopiperid-4-ones in both their preparation and physical properties makes them less attractive. For example, many of them have comparable or larger two-photon absorption cross sections, but, where reported, their fluorescence quantum yields are an order of magnitude larger than that of arylidenopiperid-4-ones. Therefore, when used as the photodynamic sensitizers they will have lower triplet-state production, since most of the excitation energy that could go into triplet state formation is lost by fluorescence.

As for materials science, compounds with a donor-bridge-acceptor motif is one of the most developed models for testing the charge transfer process in a single molecule. Recently, diferrocenylidene conjugated compounds (FcCH=CHXCH=CHFc, Fc = ferrocenyl group and linker X = O, S, CH_2, C≡C, CH=CH, C=O, PPh, P(=O)Ph and etc.) were examined for charge transport support.[11] It was found that oxygen as a linker has superior transmission characteristics.

While Klimova *et al.* were the first reporting N-methyl-2,6-(E,E)-bis(ferrocenylidene)piperid-4-one (**2**) (see Scheme 1)[12] this compound remains the only known organometallic derivative containing piperid-4-one fragment. Therefore we focused our attention on synthesis of parent complexes with different N-substituents and report synthesis, spectroscopic characterization, electrochemical properties along with structural characterization of the N-substituted 2,6-(E,E)-bis(ferrocenylidene)piperid-4-ones.

Results and discussion

Synthesis. The targeted compounds **1**–**4** were synthesized by aldol condensation reaction between ferrocenecarbaldehyde and two equivalents of N-substituted piperid-4-ones in 10% NaOH ethanol solution (Scheme 1). Isolation of complexes were carried out by column chromatography with mixtures of hexane, $CHCl_3$ and Et_2O.

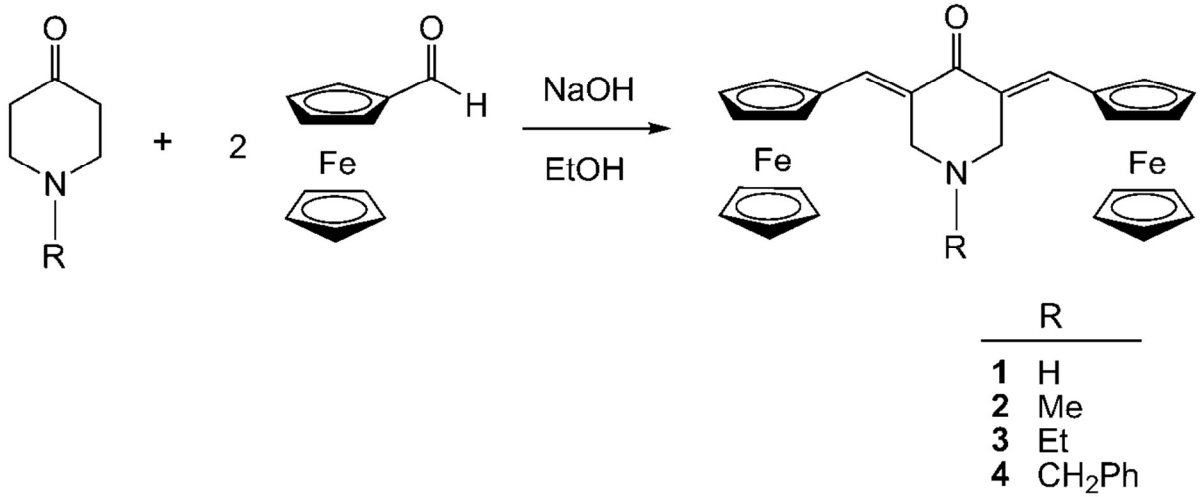

Scheme 1

The compounds **1**–**4** are red solids, air and moisture stable both in the solid state and in the solution. They have been characterized by the elemental analysis, IR, UV-vis, and NMR spectroscopy (^1H, $^{13}C\{1H\}$, see Tables S1 and S2 in Supporting information), and single-crystal X-ray diffraction analysis. The IR spectra of compounds **1**–**4** in solid state on monocrystalline ZnSe possess three absorption bands corresponding to the alkene conjugated carbonyl group in the region of 1500–1700 cm^{-1}.[13] The products are hygroscopic compounds and absorb water if allowed to stay in air.

The UV-vis spectra only slightly deviate in the series of compounds **1**–**4**, consisting of one maximum in a short-wave region around 341–348 nm and one in long-wave region 527–549 nm (Table 1). All profiles of short-wavelength maximum displayed a shoulder between 402 and 410 nm. It should be noted, that all bands of compound **1** have slight hypsochromic shift if compared to analogous bands in **2**–**4** (see Table 1). Next we compared the maxima positions for the compounds **1**–**4** (Fig. 1a, black curve) with those obtained for the model complexes: ferrocene (green curve) and 2,6-(E,E)-bis(benzylidene)piperid-4-one·HBF_4 (**5**, red curve). It clearly shows that the shape and

position of short-wave maximum for **1**–**4** only slightly deviates from that in **5** (main maximum at 329 nm in ethanol), whereas a shoulder at 402 nm and a long-wave maximum at 527 nm for **1**–**4** can be attributed to the two absorption bands of the ferrocene (323 and 442 nm). This suggestion is also supported by the fact that $\Delta\lambda$ shifts (119 and 125 nm) are almost equal between absorption bands of ferrocene and **1**. Since the piperid-4-one and ferrocene moiety behave independently in absorption spectra, we may consider them as different chromophore fragments.

Compounds **1**–**4** possess negligible fluorescence in solution. However, we detected the fluorescence band maximum at λ_{em} = 358 nm in ethanol solution of **1** when it was excited at 300 nm (Figure 1b, black curve). The maximum of this band coincides with fluorescence band maximum of ethanol solutions of **5** (Figure 1b, red curve), thus showing that the emission spectrum is dictated by fluorescence of piperid-4-one fragment. The fluorescence quantum yield for **5** was found to be 0.0031 with life time 12.53 ns. Further substitution of benzene rings on ferrocene substituents increases the probability of intersystem crossing (non-radiative decay) and/or conversion to the triplet state due to spin-orbital interaction,[14] which significantly reduces fluorescence for **1**–**4** as compared to **5**. Therefore our attempts to measure two-photon absorption spectra were unsuccessful due to extremely low quantum yields.

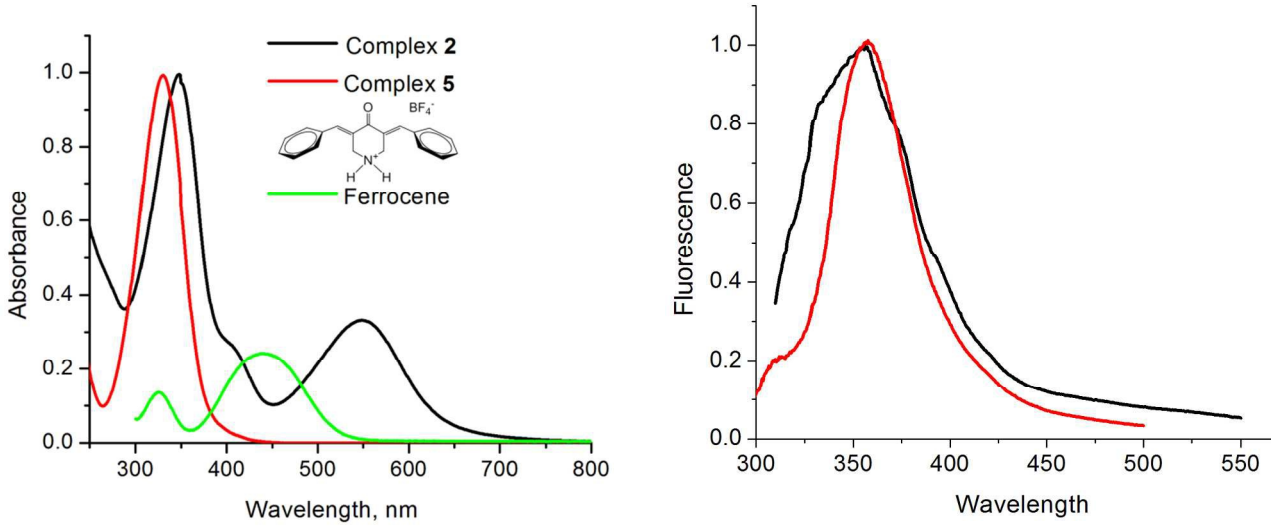

Figure 1. a) Absorption spectra (left) for compounds **2** (black), **5** (red) and ferrocene (green) b) Fluorescence spectra (right) for compounds **1** (black) and **5** (red) in ethanol. Fluorescence spectra were excited at λ_{ex} = 300 nm.

Table 1. Spectral and photophysical characteristics for compounds 1–4 and model compounds (5 and ferrocene) in methylene chloride: maximum absorption wavelength (λ_{abs}), molar absorption coefficient at the absorption maximum (ε_{max}), fluorescence maximum (λ_{em}).

Compound (R)	λ_{abs}, nm	$\varepsilon_{max}\cdot10^4$, M^{-1} cm^{-1}	λ_{em}, nm[†]
1 (R = H)	**341**[a], 402, 527	1.16	358
2 (R = Me)	**348**, 409, 549	2.19	358
3 (R = Et)	**346**, 409, 545	2.26	357
4 (R = Bz)	**347**, 410, 549	1.64	358
5	**329**[b]	3.60[†]	358
Ferrocene **6**	323, **442**[b]	0.02[†]	516

[a] Ethanol solution

[b] Main maximum in bold

Electrochemistry and spectroelectrochemistry. To check if the dimethyliden-piperidin-4-one unit allows the electronic communication between the two ferrocene moities, we have used the $[NBu_4][B(C_6F_5)_4]$ salt, which contains the weakly coordinating anion tetrakis(perfluorophenyl)borate, as inert electrolyte. In these conditions, the anodic peak-to-peak separation of subsequent oxidations usually increases.[15] All complexes undergo two overlapped ferrocene/ferrocenium oxidations, therefore, indicating the inefficiency of the electronic communication path. Also, one or two partially reversible reduction processes are present which are centred on the bridging ligand.[16] The redox potential values for **1**–**4** are collected in Table 2. In all cases, the oxidation is anodically shifted with respect to the free ferrocene, hence, the compounds are harder to oxidise suggesting that the bridging unit acts as an electron-withdrawer. At the same time the electrochemistry of complexes **1**–**4** is only apparently simple. As it is clearly evident in the cyclic voltammogram of **4** in Figure 2a, the two sharp peaks preceding the oxidation and reduction peaks are diagnostic of adsorption of the sample on the electrode surface. This phenomenon seems to be unavoidable either by changing the solvent or by changing the electrode material and is exhibited with different intensity, by all the compounds **1**–**4**. As a further example, the cyclic voltammogram of **1**, only apparently simpler than that of **4** as shown in Figure 2b, similarly hides the features of adsorption of the oxidised compound. Even if these are not well evident in the shape of the cyclic voltammogram, they are clearly put in evidence by the peak-shaped semi-integrated voltammogram, shown in the inset of Figure 2b, which is highly diagnostic for this phenomenon.[17]

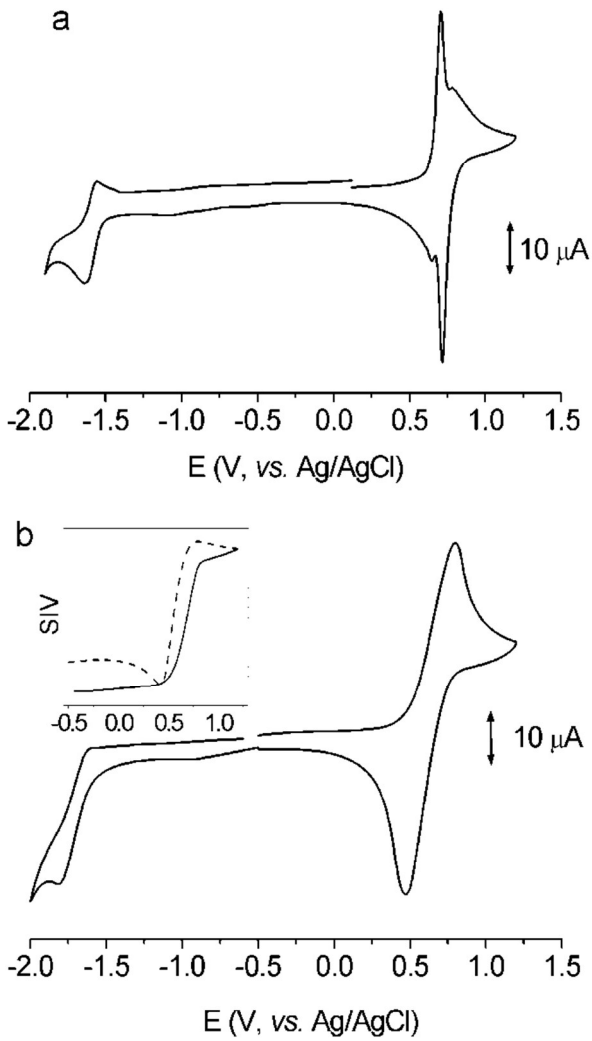

Figure 2. Cyclic voltammogram recorded at Pt electrode in CH_2Cl_2 solution of (a) complex **4** (R = Bz; $1.0 \cdot 10^{-3}$ M); (b) complex **1** (R = H; $1.2 \cdot 10^{-3}$ M), inset: semintegrated voltammogram of the anodic region. Supporting electrolyte ($[Bu_4N]B[C_6F_5]_4$ M). Scan rate 0.2 V s^{-1}.

Moreover, the second derivative of the differential pulse voltammetry of complexes **1**–**4** shows the presence of two shouldered main signals indicating of an even more complex anodic pattern (Figure 3). In fact, as it will be discussed below, bulk electrolysis and spectroelectrochemistry show that the several processes accompany the ferrocene oxidation in these complexes, which is also in agreement with the observed large peak-to-peak separation (ΔE).

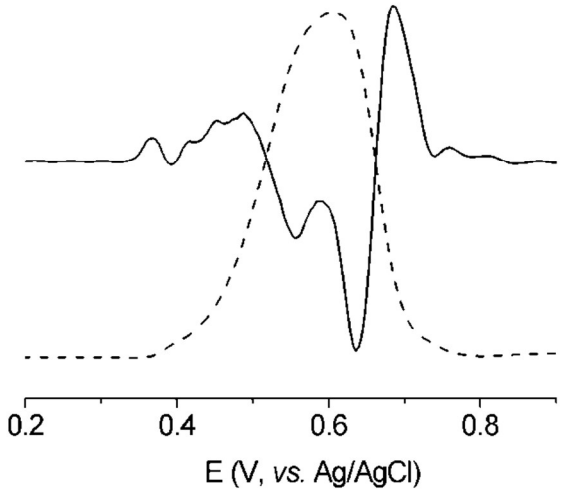

Figure 3. Differential pulse voltammetry and its 2nd derivative for complex **1** (R = H). Recorded in the same experimental conditions as those for Figure 2. Scan rate 0.02 V s^{-1}.

Table 2. Formal Electrode Potentials (V, *vs.* Ag/AgCl) and Peak-to-Peak Separations (mV) for the Redox Changes Exhibited by Complexes 1–4

Compound (R)	E'_{ox}	ΔE	E'_{Red}	ΔE	E''_{Red} [a]
1 (R = H)	+0.63	290	-1.71	210	-1.97
2 (R = Me)	+0.69	360	-1.69	230	-2.1
3 (R = Et)	+0.68	120	-1.65	130	-
4 (R = Bz)	+0.76	120	-1.60	100	-

[a] Peak potential value for irreversible process obtained by OSWV (osteryoung square wave voltammogram); Oxidation potential +0.41 V for the ferrocene in CH_2Cl_2.[18]

As it was expected, the controlled coulometry experiments for complexes **1**–**4** are also disturbed by the adsorption at the electrode surface. Nevertheless, it was confirmed that two electrons are consumed per molecule, while the cherry-red solutions turn light green. The cyclic voltammogram of the oxidized solution appears as a complementary to that of the original one. Upon reduction of the oxidized green solution a violet solution is obtained, which, once again, exhibits a cyclic voltammogram coinciding with the initial one. It should be noted that the variation of the color clearly indicates that the reversibility of the redox process is only apparent and we are in the presence of a distinct compound. Interestingly, the behavior observed in the bulk electrolysis

experiment is clearly reproduced by the UV-vis spectroelectrochemistry. The spectral data collected during the OTTLE cell spectroelectrochemistry of compounds **1**–**4** are reported in Table 3, while Figure 4 shows the spectral change observed by the stepwise removal and re-addition of two electrons to complex **4**. As an example, in this case, by removing the electrons both bands at 338 and 520 nm decreases, while the band at 520 nm is red-shifted. Also, a broad band at 750 nm appears together with a couple of bands in the UV region. The missing isosbestic point confirms that a chemical reaction occurs, accompanying the redox change. In fact, by reducing back the oxidized compound **4** a spectrum very similar, but not identical, to the original one is obtained. This behaviour is common to **1**–**4** and suggests that the chemical reaction occurs throughout the oxidation and that the new compound is stable and can be reduced back giving a compound similar, but not identical to the pristine one (Figure 5). Comparison with the colour of protonated complexes **2**·HBF_4 and **4**·HBF_4, strongly indicates that the violet solutions obtained in electrochemical experiments contain the protonated form of complexes **1**–**4**. In fact, addition of a few drops of [n-Bu_4N]OH makes the electrogenerated violet solution to turn back cherry-red. Therefore, we may conclude that protonation of N atom occurs during electrochemical experiments. One may assume that oxidation of the complexes **1**–**4** would reduce the basicity of the N atom thus making it harder to protonate. At the same time N atom is not conjugated with bis(ferrocenylidene) part of the molecule and still behaves as Lewis base which allows the protonation.

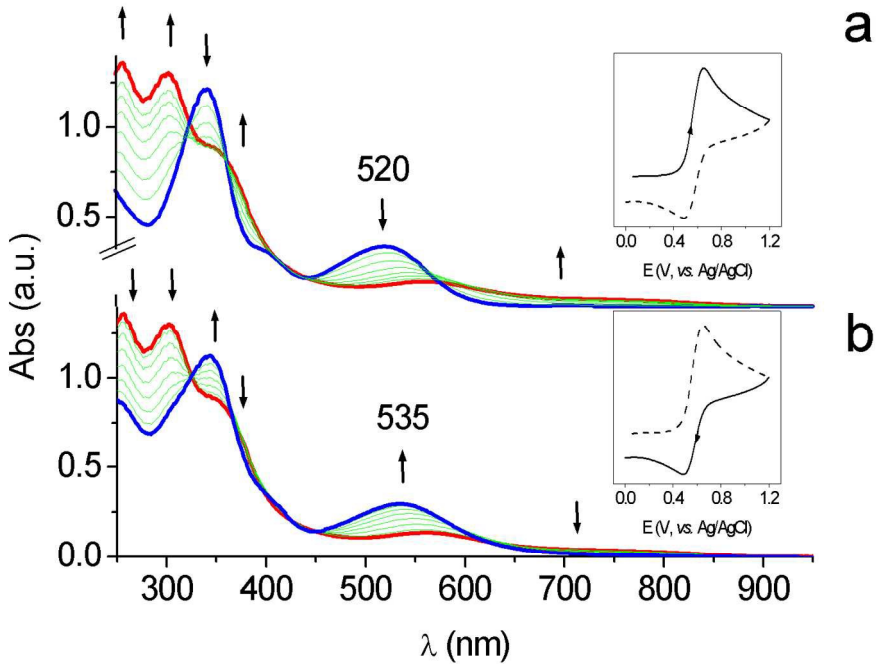

Figure 4. Spectral changes recorded in CH_2Cl_2 solution of **4** upon progressive two-electron oxidation (a) and reduction (b) in a OTTLE cell.

Table 3. Spectroscopic Changes Recorded upon Two-Electron Oxidation and Reduction of the neutral complexes 1–4.

Compound (R)	λ, nm					
1 (R=H)			341	402	519	
$\mathbf{1}^{2+}$			adsorption			
1 (reduced)			351		550	
2 (R=Me)			341	401	525	
$\mathbf{2}^{2+}$	257	303	346		563	740
2 (reduced)			348		553	
3 (R=Et)			341	400	517	
$\mathbf{3}^{2+}$	257	306	348		553	740
3 (reduced)			345		536	
4 (R=Bz)			338	400	520	
$\mathbf{4}^{2+}$	258	301	349		570	750
4 (reduced)			345		535	

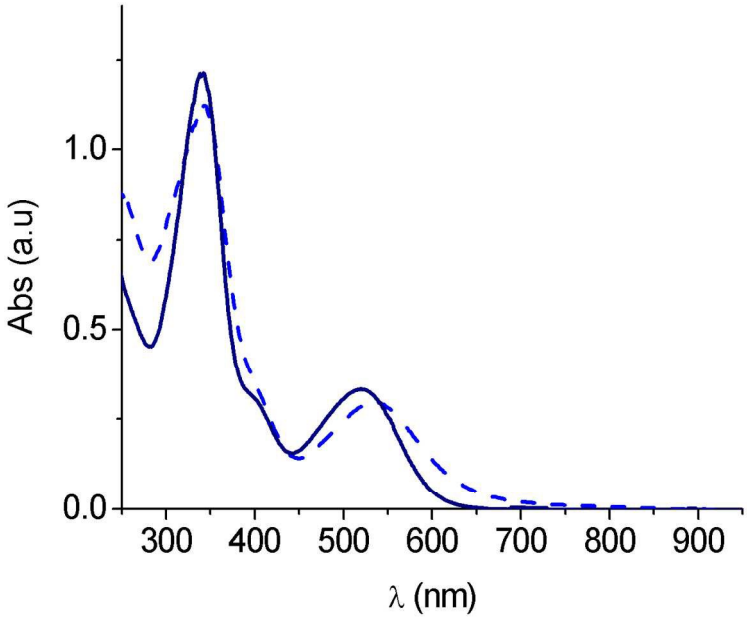

Figure 5. The absorption spectrum of complex **4** before (full line) and after (dash line) the redox cycle.

Photochemistry. A number of compounds including the chalcone type undergo photoinduced E/Z isomerisation as it was reported previously.[19] Thus we have checked the photoinduced E/Z isomerisation process in case of complex **4** by monitoring with UV-vis and NMR spectroscopy. The UV-vis spectra collected after irradiation of **4** at 520 and 400 nm are shown in Figure 6 and clearly demonstrate that both these wavelengths induce the same change in the spectrum. Moreover, the effect seems to be the same as that induced by the redox cycling, as indicated by negligible difference between spectrum obtained after the irradiation and after the redox cycle (see Figure 6, down). Having ascribed the new spectral features observed after the redox cycle to the protonation of the compounds, this result was unexpected and required additional investigation.

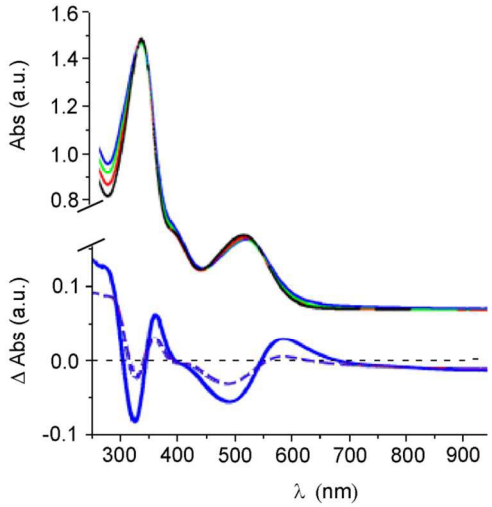

Figure 6. (up) Spectral changes recorded in CH_2Cl_2 solution of **4** upon irradiation with 520 nm light for 5 (red), 10 (green) and at 400 nm for 10 min (blue); (down) Difference spectra after the irradiation at 400 nm for 10' (dotted line) and after the redox cycle (full line).

To verify if we have either photo-induced protonation or photo-induced E/Z isomerisation for complexes **1**–**4** we decided to monitor changes by ^{1}H NMR spectroscopy (in $CDCl_3$) to detect the complex type formation during irradiation. We have chosen to monitor the effect of the irradiation at both 400 and 520 nm of solutions of complexes **1** and **4**. The irradiation of samples at 400 nm led to significant changes of their ^{1}H NMR spectra. While the major view of spectra for both complexes **1** and **4** appeared to be complicated, the positions of vinyl protons (=CH) of the ferrocenylidene moieties is informative to identify the presence in the solution of different forms. Therefore, for complex **1** we detected starting material E,E-form (7.59 ppm), and two isomerised forms the E,Z- and Z,Z forms (7.70; 7.49 and 6.97 ppm, respectively). Unfortunately, it was impossible to identify the presence of protonated forms of the complexes **1** and **4** in solution which

can be attributed by significant peak broadening for the resonances of ammonium protons. Noteworthy, that the irradiation of samples **1** and **4** at 520 nm for 16 h have not imposed any changes to their NMR spectra.

Chemical oxidation. To collect additional information about the E/Z isomerization process discussed in the spectroelectrochemistry and photochemistry sections we performed the chemical oxidation of complex **2**. Its reaction with $AgBF_4$ led to formation of tricationic product with the constitution [**2**·HBF_4][BF_4]$_2$. The suitable crystals of the oxidized compound were grown for X-ray diffraction analysis but appeared to be of poor quality to further discuss the bond lengths and angles. At the same time, It was found that the unit cell contain three anions of BF_4 and one trication [**2H**]$^{3+}$ as its E,E isomer. Two BF_4 anions are present as a counter-ion for the oxidized ferrocene moieties and one for the protonated N atom. Even though we were able to collect the diffraction data for only E,E isomer it is impossible to rule out the formation of the E,Z or Z,Z isomers because during crystallization process these forms can convert back to the more thermodynamically stable E,E form or not crystallized at all. Therefore we can conclude that the protonation of N atom occurs during either chemical or electrochemical experiments due to the presence of water molecules in the samples as a source of protons, which in turn is also accompanied by E/Z isomerisation process.

X-Ray diffraction study. In order to confirm the structures in the solid state we performed the X-ray diffraction studies for **2** and **3** (Figure 7, for compound **3**). These compounds crystallize in non-centrosymmetrical group $P2_1$ and thus are demonstrating their potential ability to be used as non linear optical (NLO) or THz generating materials. Also, crystal structures of salts **2**·HBF_4 and **4**·HBF_4 (Figures 8 and 9) were obtained for the protonated forms of compounds **2** and **4**. The compound **2**·HBF_4 crystallizes simultaneously in two polymorph modifications triclinic (plates) and monoclinic (prisms). Both polymorphs for **2**·HBF_4 were obtained in one vial. The crystal structure of the triclinic form of **2**·HBF_4 contains two independent molecules (A and B) in the asymmetric unit. The bond lengths and angles in both polymorphs are very similar (see Table 4). The Fe1- and Fe2-bound cyclopentadienyl rings are eclipsed and staggered, respectively, for molecule A, while for molecule B only eclipsed conformation observed. The independent molecules A and B in triclinic form are found to be different conformational isomers of the first and second type, respectively (*vide infra*).

All major structural characteristics for all obtained crystals repeat those reported for **2**,[13] analogous N-alkylated piperid-4-ones[20] and could be summarized as follows: 1) the ferrocenyl moieties were found in *trans*-position with respect to carbonyl group C1=O1 showing that

compounds crystallize as E,E-isomers; 2) the Fe···centroid distances to the substituted η^5-C_5H_4 ring are slightly shorter than those for the η^5-C_5H_5 ring, which is in accordance with other monosubstituted ferrocenes; 3) the envelope conformation was observed for piperid-4-one central unit; 4) the nitrogen atom possesses the pyramidal geometry in all compounds with sum of the angles about 330° (see Table 4); 5) the N1 atom deviates by 0.677(4)–0.719(4) Å from the plane defined by C1 to C5 atoms; 6) the mean value for double bonds C2–C6 and C5–C8 conjugated with carbonyl group 1.348(6) Å is consistent with statistically observed 1.340 Å;[21] 7) the mean N–C bond distance of 1.469 Å for **2** and **3** was found to be somewhat shorter 1.469 Å than for protonated compounds **2**·HBF_4 and **4**·HBF_4

It is interesting to note that two ferrocene moieties occupy different position relative to the piperid-4-one unit and N1 atom inversion with respect to the planar central unit leading to the three types of the rotational isomers: 1) N1 atom inverted on the same side with *syn*-facial disposition of ferrocene ligands (triclinic form of **2**·HBF_4 molecule A, see Figure 8); 2) N1 atom inverted on the opposite side with *syn*-facial disposition of the ferrocene ligands (**2**, **3**, triclinic form of **2**·HBF_4 molecule B, and monoclinic form of **2**·HBF_4, see Figure 7 and 8); 3) *trans*-disposition of the ferrocene ligands (**4**·HBF_4, see Figure 9).

Here, all three types of isomers were structurally characterized. Since the enthalpic penalty between *trans* and *syn*-facial oriented isomers was reported about 0.7 kcal/mol,[13] one may conclude that the weak noncovalent intermolecular or intramolecular interactions may serve as the driving force for the isomer type formation during crystallization. Apparently, the crystal packing of the neutral compounds **2** and **3** is dictated by C–H···O hydrogen bonds between ferrocene and carbonyl moieties leading to the chain type structures along crystallographic axis *a*. In case of monoclinic form **2**·HBF_4 rotational isomer type two is formed due to N–H···O and antiparallel carbonyl···carbonyl interactions [C1···C1A (– x, 1 – y, 1 – z) = 3.315(3) Å, O1–C1···C1A = 88.7(8)°] leading to the dimer type structure between two neighboring cations (Figure 10) while C–H···F interactions generate a three-dimensional network. The triclinic form of compound **2**·HBF_4 contains both isomers of type one (A molecule) and type two (B molecule). Again, the type two isomer shows N–H···O whereas for the type one N–H···F hydrogen bonds observed besides a number of C–H···F hydrogen bonds present for both molecules. The crystal packing for **4**·HBF_4 contains the system of C–H···F and N–H···F hydrogen bonds, and short intramolecular C–H···π interaction between the benzyl carbon atoms and ferrocene C–H bond (C24–H24···bond centroid(C31–C32) = 2.89 Å) which leading to the formation of the third type rotational isomer. The molecules in **4**·HBF_4

arranged in linear infinite chain along crystallographic axis *b* (Figure 11). For hydrogen bond Table S4, see Supporting information.

Table 4. Selected geometric parameters (Å and °) for **2**, **3**, and salts **2**·HBF_4 and **4**·HBF_4

	2	**3**	**2**·HBF_4 (Triclinic)		**2**·HBF_4	**4**·HBF_4
			A	B	(Monoclinic)	
N1–C3	1.462(4)	1.451(8)	1.509(7)	1.505(5)	1.493(3)	1.465(8)
N1–C4	1.462(4)	1.454(8)	1.527(6)	1.484(6)	1.499(3)	1.502(8)
N1–C7	1.458(5)	1.480(8)	1.458(9)	1.486(5)	1.499(3)	1.523(8)
C1–O1	1.218(5)	1.225(7)	1.237(5)	1.225(5)	1.240(3)	1.235(7)
C5–C8	1.349(4)	1.352(8)	1.353(6)	1.344(6)	1.349(3)	1.344(8)
C2–C6	1.347(5)	1.346(8)	1.349(6)	1.343(5)	1.356(3)	1.326(9)
Fe1···Cg1[a]	1.644(2)	1.662(3)	1.651(2)	1.643(2)	1.639(1)	1.641(3)
Fe1···Cg2[a]	1.656(2)	1.660(3)	1.656(2)	1.654(3)	1.651(1)	1.652(4)
Fe2···Cg3[a]	1.651(2)	1.668(3)	1.651(2)	1.650(2)	1.643(1)	1.653(2)
Fe2···Cg4[a]	1.654(2)	1.668(3)	1.656(2)	1.659(3)	1.650(1)	1.658(3)
C3–N1–C4	110.5(3)	111.8(5)	108.5(4)	111.9(3)	110.28(19)	112.4(5)
C3–N1–C7	109.8(3)	112.0(5)	111.1(4)	110.1(3)	110.6(2)	111.7(5)
C4–N1–C7	110.5(3)	113.1(5)	112.8(5)	111.5(4)	110.62(19)	110.9(5)

[a] Cg = centroid where 1 (C9 to C13), 2 (C14 to C18), 3 (C19 to C23), and 4 (C24 to C28)

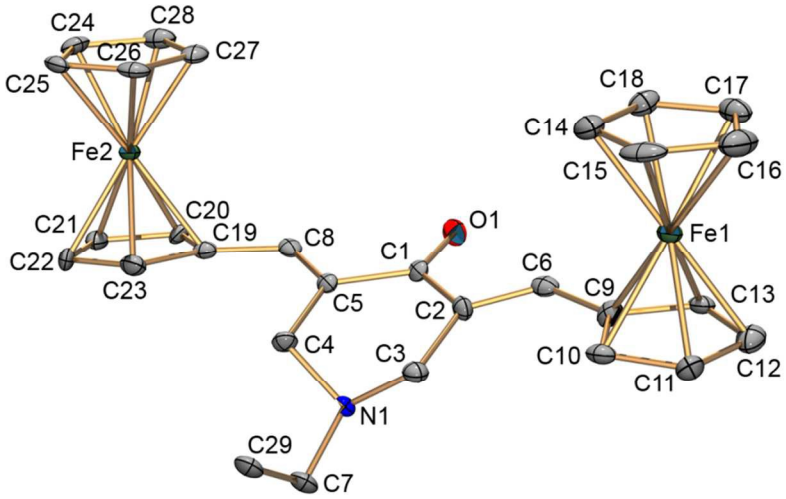

Fig. 7. The structure of compound **3**. Ellipsoids are shown at the 50% level. Hydrogen atoms are omitted for clarity.

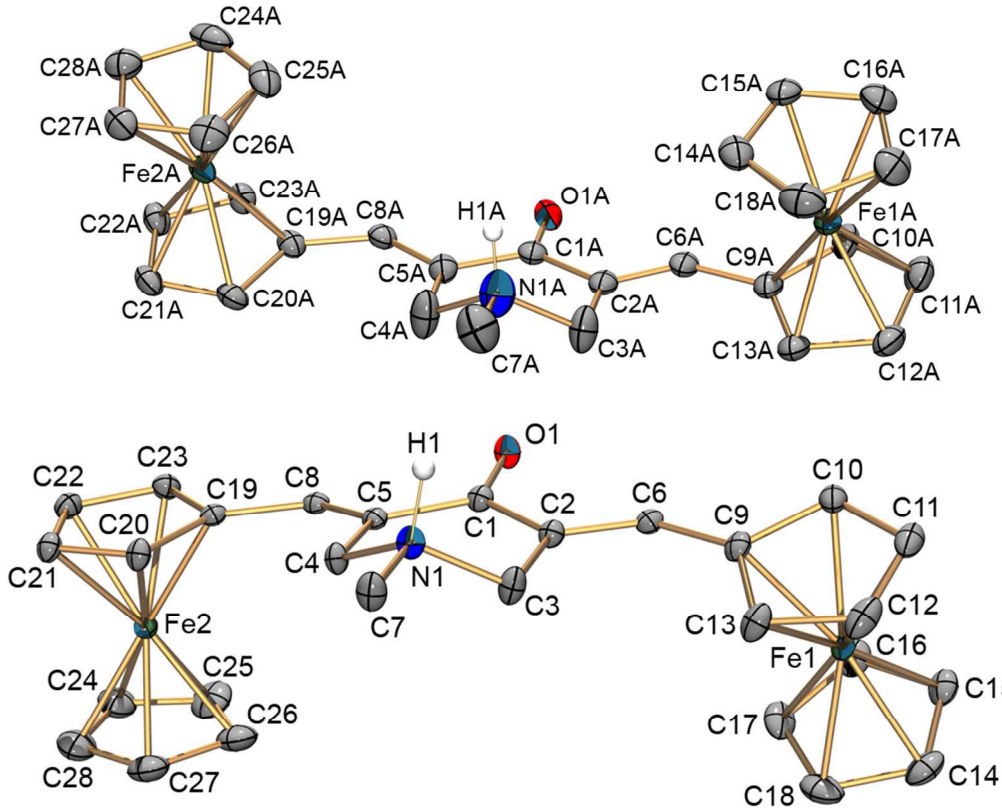

Figure 8. The structure of two polymorph modifications for compound **2**·HBF_4: independent molecule A of triclinic form (up) and monoclinic form (down) showing rotational isomers. Ellipsoids are shown at the 50% level. Hydrogen atoms are omitted for clarity with exception for N–H.

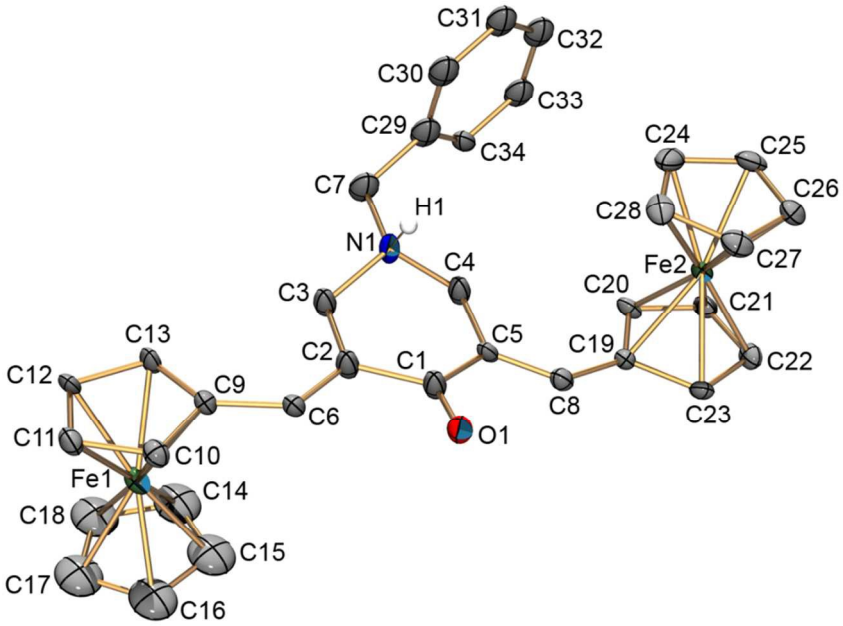

Figure 9. The structure of compound **4**·HBF_4. Ellipsoids are shown at the 50% level. Hydrogen atoms are omitted for clarity with exception for N–H.

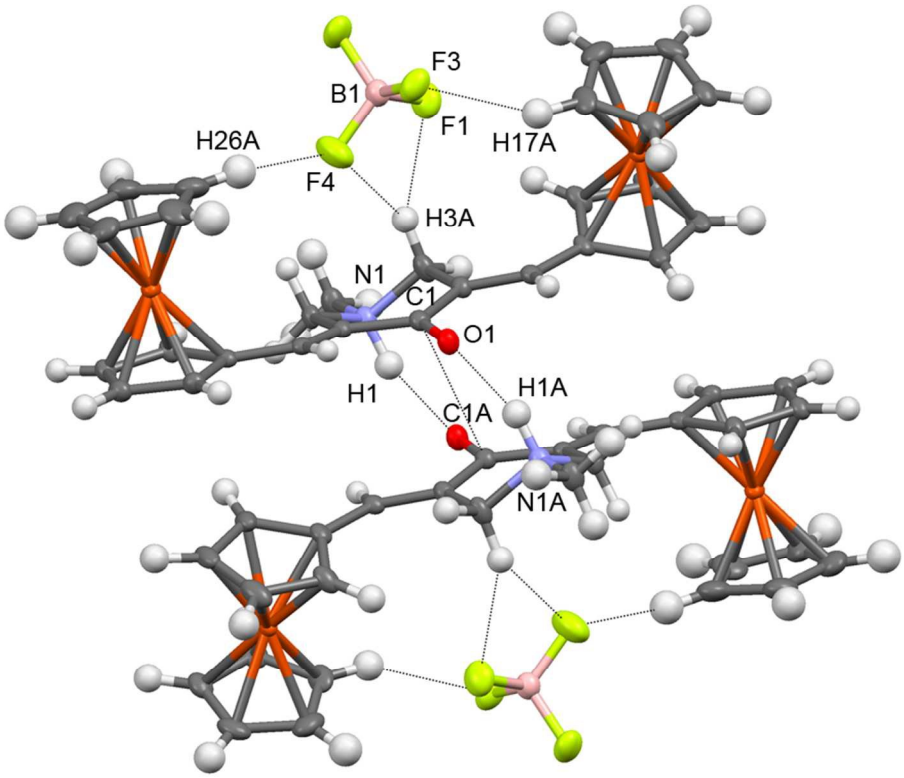

Figure 10. View of a dimer with two anions for monoclinic form of **2**·HBF_4. Symmetry code (A): (– x, 1 – y, 1 – z; dashed lines indicate the antiparallel π(CO)···π(CO), N–H···O and C–H···F interactions.

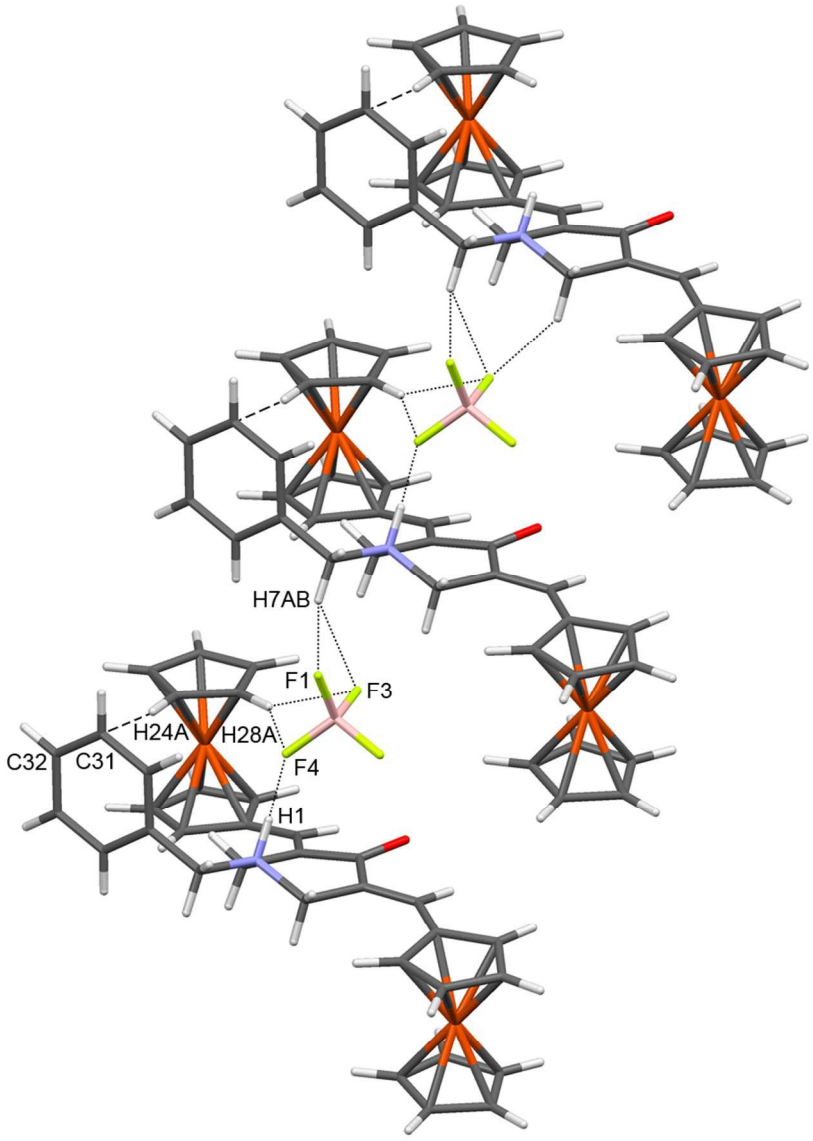

Figure 11. View of a stack of **4**·HBF_4. Symmetry code (AB): (x, –1 + y, z); dashed lines indicate the intramolecular and intermolecular N–H···F and C–H···F hydrogen bonds and weak C–H···π interactions.

Conclusion

The aldol condensation allowed to obtain selectively four N-substituted 2,6-(E,E)-bis(ferrocenylidene)piperid-4-ones with high yields. Comparison of the UV-vis maxima positions for all complexes with model compounds shows that the piperid-4-one unit and ferrocene moieties behave independently in the absorption spectra and may considered as the different chromophore fragments. The structure of the three predicted conformational isomers were experimentally

confirmed with X-ray diffraction analysis showing *trans*- and *syn*-facial disposition of the ferrocene moieties and inversion of the nitrogen atom. The different type of isomer formation dictates by specific inter- and intramolecular type of contacts in the solid state. It was found that the two-electron oxidation leads to intensity decrease of bands at 338 and 520 nm, red-shift of the band at 520 nm, and a new broad band at 750 nm which is characteristic to the ferricinium moieties. The protonation of N-atom and chemical or electrochemical induced E/Z isomerization occur simultaneously according to UV-vis, ^{1}H NMR spectroscopy and X-ray diffraction data for complexes **1**–**4**.

Experimental Section

General Procedures. All reactions were carried out under argon in anhydrous solvents purified and dried using standard procedures. The column chromatography was conducted in argon atmosphere. Silica gel (230-400 mesh) was purchased from Alfa Aesar. Silica gel was dried at 180 °C and 0.01 mm Hg vacuum after which filled with argon at ambient temperature for column chromatography. The ^{1}H and ^{13}C NMR spectra were recorded either on a Bruker AMX-300 spectrometer or on Bruker Advance DPX400. Chemical shifts are given in ppm relative to either residual protons of the solvent ($CDCl_3$ δ = 7.25 (^{1}H) and 77.0 (^{13}C)) or Me_4Si for ^{1}H and ^{13}C spectra. The IR spectra of the solid compounds were measured by Thermo Nicolet Magna IR 550 FTIR spectrometer on monocrystalline ZnSe over the range 400–4000 cm^{-1}. The UV-vis spectra were measured on spectrophotometer Varian Cary 100 Scan in methylene chloride solution (l = 0.1 cm) with concentrations 5–6·10^{-4} M for **1**–**4** and in ethanol for **5** and ferrocene with concentrations 2·10^{-2} M. The fluorescence spectra were recorded on spectrofluorometer Horiba Jobin Yvon Fluorolog 3-221 in ethanol solutions at a right angle in 1 cm cuvette. The method used to determine fluorescence quantum yields (φ) is based on using 9,10-diphenylanthracene (φ = 0.9) as a standard and **5** in concentration 10^{-6} M.[22] Fluorescence lifetimes (τ) were measured with laser diode excitation (λ = 293 nm) with pulse duration time less than 100 ps. Electrochemistry has been studied by using nitrogen-saturated CH_2Cl_2 solutions of the compounds under study with $[NBu_4][B(C_6F_5)_4]$ (0.1 M) as supporting electrolyte. CH_2Cl_2 was freshly distilled and $[NBu_4][B(C_6F_5)_4]$ was freshly prepared by metathesis of $Li[B(C_6F_5)_4]\cdot 2Et_2O$ (Boulder Scientific Co., Boulder, CO) with $[NBu_4]Cl$ as described elsewhere.[15] Cyclic voltammetry was performed in a three-electrode cell containing a platinum working electrode, a platinum counter electrode and AgCl (KCl 3M) reference electrode.

A BAS 100W electrochemical analyzer was used as polarizing unit. Controlled potential coulometry was performed in an H-shaped cell with anodic and cathodic compartments separated by a sintered-glass disk. The working macroelectrode was a platinum gauze; a mercury pool was used as the counter electrode and a calomel electrode as reference. The UV−vis spectroelectrochemical measurements were carried out using a Perkin-Elmer Lambda 2 UV−vis spectrophotometer and an OTTLE (optically transparent thin-layer electrode) cell equipped with a Pt-minigrid working electrode (32 wires/cm), Pt minigrid auxiliary electrode, Ag wire pseudoreference and CaF_2 windows.[23] Working potential was kept fixed at the peak potential of the process under study and spectra were progressively collected after every 2 min of electrolysis.

Synthesis of cis-2,6-(E,E)-bis(ferrocenylidene)-4-piperidone (1). In a 50 ml round bottom flask, 4-piperidone monohydrate hydrochloride 0.275 g (2.34 mmol) was added into 20 ml of 10% NaOH solution followed by adition of ferrocenecarboxaldehyde 1.001 g (4.67 mmol). The red reaction mixture allowed stirring overnight after which red precipitate formed. The reaction mixture was poured into 200 ml of water, filtered through the fritted funnel with filter paper and washed with 50 ml of water. The residue was dissolved in 70 ml of CH_2Cl_2 and dried with small amount of silica gel. The column chromatography (2/10 cm) was performed under inert atmosphere. Elution with 50:10 ml of hexane:ethylacetate mixture gave light red fraction and mixture 10:60ml ethylacetate:dichloromethane gave dark-red fraction of product. The second fraction was dried to give red solid 0.911 g. Yield 79%. Anal. calcd. for $C_{27}H_{25}Fe_2NO$ (491.06): C 65.98, H 5.13, N 2.85. Found C 66.23, H 5.31, N 2.75. IR (ZnSe, cm^{-1}): ν = 1658, 1606, 1563.

cis-2,6-(E,E)-bis(ferrocenylidene)-N-methyl-4-piperidone ***(2)*** was obtained analogously to **1** from 4-methylpiperidone 0.276 g (2.44 mmol) and ferrocenecarboxaldehyde 1.003 g (4.68 mmol). Red solid. Yield: 0.949 g (77%). Anal. calcd. for $C_{28}H_{27}Fe_2NO$ (505.07): C 66.52, H 5.39, N 2.77. Found C 66.61, H 5.46, N 2.73. IR (ZnSe, cm^{-1}): ν = 1663, 1606, 1564.

cis-2,6-(E,E)-bis(ferrocenylidene)-N-ethyl-4-piperidone ***(3)*** was obtained analogously to **1** from 4-ethylpiperidone 0.296 g (2.32 mmol) and ferrocenecarboxaldehyde 1.001 g (4.67 mmol). Red solid. Yield: 0.943 g (78%). Anal. calcd. for $C_{29}H_{29}Fe_2NO$ (519.09): C 67.04, H 5.63, N 2.70. Found C 67.21, H 5.81, N 2.51. IR (ZnSe, cm^{-1}): ν = 1662, 1609, 1560.

cis-2,6-(E,E)-bis(ferrocenylidene)-N-benzyl-4-piperidone ***(4)*** was obtained analogously to **1** from 4-benzylpiperidone 0.503g (2.65 mmol) and ferrocenecarboxaldehyde 1.136 g (5.31 mmol). Purple solid. Yield: 1.247 g (81%). Anal. calcd. for $C_{34}H_{31}Fe_2NO$ (581.11): C 70.21, H 5.38, N 2.41. Found C 70.39, H 5.54, N 2.33. IR (ZnSe, cm^{-1}): ν = 1663, 1604, 1563.

Synthesis of 2·HBF_4**.** To red solution of complex **2** 0.196 g (0.39 mmol) in wet MeCN (12 ml with 2% of water) was added $AgBF_4$·3dioxane 0.185 g (0.39 mmol). Solution immediately turned purple and precipitation of silver residue was observed. The purple suspension was allowed stirring for 5 h. The silver residue was centrifuged, purple solution was decanted and concentrated to ca. 3 ml. Crystallization by diffusion of Et_2O vapors into purple MeCN solution led to formation of black prisms and plates of the product. Mother solution was decanted and crystals were dried in vacuum. Yield 0.160 g (71%). Anal. calcd. for $C_{27}H_{26}BF_4Fe_2NO$ (578.99): C 56.01, H 4.53, N 2.42. Found C 56.33, H 4.67, N 2.49.

Synthesis of 3·HBF_4 was obtained analogously to **2**·HBF_4 from complex **3** 0.155 g (0.3 mmol) and $AgBF_4$·3dioxane 0.138 g (0.3 mmol). Black solid. Yield 0.142 g (78%). Anal. calcd. for $C_{29}H_{30}BF_4Fe_2NO$ (607.04): C 57.38, H 4.98, N 2.31. Found C 57.42, H 5.05, N 2.38.

Synthesis of 4·HBF_4 was obtained analogously to **2**·HBF_4 from complex **4** 0.203 g (0.35 mmol) and $AgBF_4$·3dioxane 0.160 g (0.35 mmol). Black solid. Yield 0.168 g (72%). Anal. calcd. for $C_{34}H_{32}BF_4Fe_2NO$ (669.11): C 61.03, H 4.82, N 2.09. Found C 61.29, H 4.95, N 2.19.

Oxidation of complex 2. Under argon atmosphere complex **2** 0.196 g (0.39 mmol) was dissolved in dry CH_2Cl_2 (8 ml) in a Schlenck flask. To red solution was added $AgBF_4$·3dioxane 0.370 g (0.79 mmol). Solution immediately turned emerald green and precipitation of silver residue was observed. The green suspension was allowed stirring for 3 h. Solution was filtered under argon and concentrated to ca. 4 ml. Crystallization by layering the green CH_2Cl_2 solution with excess of Et_2O led to formation of black prisms of the product suitable for X-ray crystallography. Yield 0.120 g (41%). Anal. calcd. for $C_{27}H_{26}B_3F_{12}Fe_2NO$ (752.60): C 43.09, H 3.48, N 1.86. Found C 43.75, H 3.99, N 2.25.

X-Ray Diffraction Study. The crystals of the compounds **2** and **3** were grown up by slow diffusion of hexane into their ethylacetate solution in a desiccator. The crystals of salts **2**·HBF_4 and **4**·HBF_4 were obtained by slow diffusion of Et_2O vapors into solution of complexes **2** or **4** in CH_2Cl_2 containing equimolar amount of HBF_4·Et_2O under inert atmosphere. The BF_4 anions for triclinic form of **2**·HBF_4 and **4**·HBF_4 were disordered over two positions with equal occupancies. The unit cell of **4**·HBF_4 contain severely disordered CH_2Cl_2 crystallization molecules which contribution were removed from the diffraction data with PLATON/SQUEEZE instruction[24,25] for the final refinement. The principal crystallographic data and refinement parameters are listed in Table S3 (see supporting information). X-ray diffraction experiments were carried out with a Bruker Apex II CCD area detector, using graphite monochromated Mo K_α radiation (λ = 0.71073 Å) at 100 K. Absorption corrections were applied semi-empirically using APEX2 program.[26] The structures were solved by

direct methods and refined by the full-matrix least-squares against F^2 in an anisotropic (for non-hydrogen atoms) approximation. All hydrogen atom positions were refined in isotropic approximation in "riding" model with the $U_{iso}(H)$ parameters equal to 1.2 $U_{eq}(C_i)$, for methyl groups equal to 1.5 $U_{eq}(C_{ii})$, where $U(C_i)$ and $U(C_{ii})$ are respectively the equivalent thermal parameters of the carbon atoms to which the corresponding H atoms are bonded. All calculations were performed using the SHELXTL software.[27]

CCDC-1049832 (for **2**), -1049835 (for **3**), -1049834 (for triclinic **2**·HBF_4), -1049833 (for monoclinic **2**·HBF_4), and -1049836 (for **4**·HBF_4) contain the supplementary crystallographic data for this paper. These data can be obtained free of charge from The Cambridge Crystallographic Data Centre via www.ccdc.cam.ac.uk/data_request/cif.

Associated Content

Supporting Information

Crystallographic information (in cif format) for compounds **2**, **3**, **2**·HBF_4 and **4**·HBF_4, and Tables S1–S4.

Author Information

Alexander Romanov, e-mail: asromanov5@gmail.com

Fabrizia Fabrizi de Biani, e-mail: fabrizi@unisi.it

Acknowledgments

A.S.R. and T.V.T. were supported by NSF grant DMR-0934212 (PREM).
This article is dedicated in memoriam to Professor Mikhail Yu. Antipin.

For table of contents use only

Synthesis, Properties and Polymorph Structures of the Conformational Isomers of N-substituted 2,6-(E,E)-bis(ferrocenylidene)piperid-4-ones

Alexander S. Romanov, Gary F. Angles, Alexey V. Shapovalov, Fabrizia F. Fabrizi de Biani, Maddalena Corsini, Stefania Fusi, Tatiana V. Timofeeva

References

[1] J. March, *Advanced Organic Chemistry*, Wiley, New York, 1992.

[2] (a) L.R. Ferguson, M. Philpott, *Curr. Cancer Drug Targets,* 2007, 459; (b) S. Singh, A. Khar, *Anticancer Agents Med. Chem*., 2006, 259 (and references therein).

[3] (a) K.M. Youssef, M.A. El-Sherbeny, F.S. El-Shafle, H.A. Farag, O.A. Al-Deeb, S.A.A. Awadalla, *Arch. Pharm. Chem. Med. Chem*., 2004, **337**, 42; (b) W.J. Gufford, K.J. Shaw, J.L. Dallas, S. Koovakkat, W. Lee, A. Liang, D.R. Light, M.A. McCarrick, M. Whitlow, B. Ye, M.M. Morrissey, *J. Med. Chem.*, 1999, **42**, 5415; (c) J.R. Dimmock, M.P. Padmanilayam, G.A. Zello, K.H. Nienaber, T.M. Allen, C.L. Santos, E. De Clercq, J. Balzarini, E.K. Manavathu, J.P. Stables, *Eur. J. Med. Chem.*, 2003, **38**, 169.

[4] I.L. Odinets, O.I. Artyushin, E.I. Goryunov, K.A. Lyssenko, E.Yu. Rybalkina, I.V. Kosilkin, T.V. Timofeeva, M.Yu. Antipin, *Heteroatom Chem.*, 2005, **16**, 497.

[5] (a) M.V. Makarov, E.S. Leonova, E.V. Matveeva, E.Yu. Rybalkina, G.-V. Röschenthaler, T.V. Timofeeva, I.L. Odinets, *Phosphorus, Sulfur, and Silicon and the Related Elements*, 2011, **186**, 908 (and references therein); (b) U. Das, R.K. Sharma, J.R. Dimmock, *Curr. Med. Chem.*, 2009, **16**, 2001-2020, (c) Adams, B. K.; Cai, J.; Armstrong, J.; Herold, M.; Lu, Y. J.; Sun, A.; Snyder, J. P.; Liotta, D. C.; Jones, D. P.; Shoji, M. *Anti-Cancer Drugs,* 2005, **16**, 263; (d) Subramaniam, D.; May, R.; Sureban, S. M.; Lee, K. B.; George, R.; Kuppusamy, P.; Ramanujam, R. P.; Hideg, K.; Dieckgraefe, B. K.; Houchen, C. W.; Anant, S. *Cancer Res*., 2008, **68**, 1962; (e) Selvendiran, K.; Tong, L.; Vishwanath, S.; Bratasz, A.; Trigg, N. J.; Kutala, V. K.; Hideg, K.; Kuppusamy, P., *J. Biol. Chem.,* 2007, **282**, 28609.

[6] (a) T. Kalai, M.L. Kuppusamy,M. Balog, K. Selvendiran, B.K. Rivera, P. Kuppusamy, K. Hideg, *J. Med. Chem.,* 2011, **54**, 5414; (b) K.M. Youssef, M.A. El-Sherbeny, F.S. El-Shafle, H.A. Farag, O.A. Al-Deeb, S.A.A. Awadalla, *Arch. Pharm. Med. Chem*., 2004, **337**, 42.

[7] (a) S. Kumar, U. Narain, K. Misra, *Bioconjug. Chem.,* 2001, **12**, 464; (b) U. Das, S. Das, B. Bandy, J.P. Stables, J.R. Dimmock, *Biorg. Med. Chem.,* 2008, **16**, 3602.

[8] U. Das, H. N. Pati, H. Sakagami, K. Hashimoto, M. Kawase, J. Balzarini, E. De Clercq, J.R. Dimmock, *J. Med. Chem.*, 2011, **54**, 3445.

[9] (a) Spangler, C. W.; Starkey, J. R.; Meng, F.; Gong, A.; Drobizhev, M.; Rebane, A.; Moss, B., *Proc. SPIE***,** 2005, **5689**, 141; (b) Morone, M.; Beverina, L.; Abbotto, A.; Silvestri, F.; Collini, E.; Ferrante, C.; Bozio, R.; Pagani, G. A., *Organic Lett.,* 2006, **8**, 2719; (c) Arnbjerg, J.; Jiménez- Banzo, A.; Paterson, M. J.; Nonell, S.; Borrell, J. I.; Christiansen, O.; Ogilby, P. R., *J.*

Amer. Chem. Soc., 2007, **129**, 5188; (d) Dy, J. T.; Ogawa, K.; Satake, A.; Ishizumi, A.; Kobuke, Y., *Chem. Eur. J.,* 2007, **13**, 3491.

[10] (a) Rumi, M.; Ehrlich, J. E.; Heikal, A. A.; Perry, J. W.; Barlow, S.; Hu, Z.; McCord-Maughon, D.; Parker, T. C.; Röckel, H.; Thayumanavan, S.; Marder, S. R.; Beljonne, D.; Brédas, J.-L., *J. Am. Chem. Soc*., 2000, **122**, 9500; (b) Chung, S.-J., Rumi; M., Alain, V.; Barlow, S.; Perry, J. W.; Marder, S. R., *J. Am. Chem. Soc*,. 2005, **127**, 10844; (c) Chung, S.-J.; Zheng, S.; Odani, T.; Beverina, L.; Fu, J.; Padilha, L. A.; Biesso, A.; Hales, J. M.; Zhan, X.; Schmidt, K.; Ye, A.; Zojer, E.; Barlow, S.; Hagan, D. J.; Van Stryland, E. W.; Yi, Y.; Shuai, Z.; Pagani, G. A.; Brédas, J.-L.; Perry, J. W.; Marder, S. R., *J. Am.. Chem. Soc*., 2006, **128**, 14444.

[11] Y. Li, M. Josowicz, L.M. Tolbert, *J. Am. Chem. Soc*., 2010, **132**, 10374 (and references therein).

[12] E.I. Klimova, M.M. García, T.K. Berestneva, C.A. Toledano, R.A. Toskano, L.R. Ramírez, *J. Organomet. Chem.*, 1999, **585**, 106.

[13] V.V. Nesterov, V.N. Nesterov, M.G. Richmond, *Polyhedron*, 2012, **35**, 124.

[14] K.N. Solovev, E.A. Borisevich, *Phys. Usp*., 2005, **48**, 247.

[15] R. J. LeSuer, W. E. Geiger, *Angew. Chem., Int. Ed.,* 2000, **39**, 248.

[16] (a) E. Klimova, T. Klimova, J.M. Martínez Mendoza, L. Ortiz-Frade, J.-L. Maldonado, G. Ramos-Ortíz, M. Flores-Alamo, M.M. García, *Inorganica Chimica Acta*., **2009**, 362, 2820; (b) Y. Li, M. Josowicz, L.M. Tolbert, *J. Am. Chem. Soc*., 2010, **132**, 10374.; (c) S. Easwaramoorthi, B. Umamahesh, P. Cheranmadevi, R.S. Rathorec, K.I. Sathiyanarayanan, *RSC Adv*., 2013, **3**, 1243.

[17] M.O. Bernard, C. Bureau, J.M. Soudan, G. Lfcayon, *J. Electroanal. Chem.*, 1997, **431**, 153

[18] Zanello, P. *Inorganic Electrochemistry: Theory, Practice and Application*; RSC: Oxford, U.K., 2003.

[19] (a) D.I. Schuster. "The photochemistry of enones". In The Chemistry of Enones. S. Patai and Z. Rappoport, Eds. John Wiley & Sons, Chichester, U.K., 1989, 623; (b) P. Perjési1, M. Takács, E. Ösz, Z. Pintér, J. Vámos, K. Takács-Novák, *J. Chromatogr. Sc.*, 2005, **43**, 289; (c) W.J. Lee, J.C. Lim, S.-H. Paek, K. Song, *Kor. Pol. J.*, 2001, **9**, 339.

[20] (a) V.N. Nesterov, T.V. Timofeeva, S.S. Sarkisov, A. Leyderman, C.Y.C. Lee, M.Y. Antipin, *Acta Crystallogr., Sect. C,* 2003, **59**, 605; (b) Z. Jia, J.W. Quail, V.K. Arora, J.R. Dimmock, *Acta Crystallogr., Sect. C,* 1989, **45**, 285, 1117; (c) P. Tongwa, T.L. Kinnibrugh, G.R. Kicchaiahgari, V.N. Khrustalev, T.V. Timofeeva, *Acta Crystallogr., Sect. C,* 2009, **65**, 155; (d) A. Fonari, E.S.

Leonova, M.V. Makarov, I.S. Bushmarinov, I.L. Odinets, M.S. Fonari, M.Yu. Antipin, T.V. Timofeeva, *J. Mol. Struct*., 2011, **1001**, 68.

[21] F.H. Allen, O. Kennard, D.G. Watson, L. Brammer, A.G. Orpen, R. Taylor, *J. Chem. Soc. Perkin Trans. II*, 1987, S1.

[22] (a) S.Hamai, F.Hirayama, *J. Phys. Chem*., 1983, **87**, 83; (b) Maciejewski, A.; Steer, R. P. *J. Photochem.*, 1986, **35**, 59.

[23] M. Krejcĭk, M..F. Daněk, F. Hartl, *J. Electroanal. Chem.*, 1991, **317**, 179.

[24] A. L. Spek, *Acta Cryst.* D, 2009, **65**, 148.

[25] P. Sluis, A. L. van der & Spek, *Acta Cryst.* A, 1990, **46**, 194.

[26] Bruker (2005), APEX2 software package, Bruker AXS Inc., 5465, East Cheryl Parkway, Madison, WI 5317.

[27] Sheldrick, G. M. (2001). SHELXTL-NT. Version 6.12. Bruker AXS Inc., Madison, Wisconsin, USA.

Graphical abstract for: Structures of the Conformational Isomers and Polymorph Modifications of N-substituted 2,6-(E,E)-bis(ferrocenylidene)piperid-4-ones. Photo- and electrochemically induced E/Z isomerization

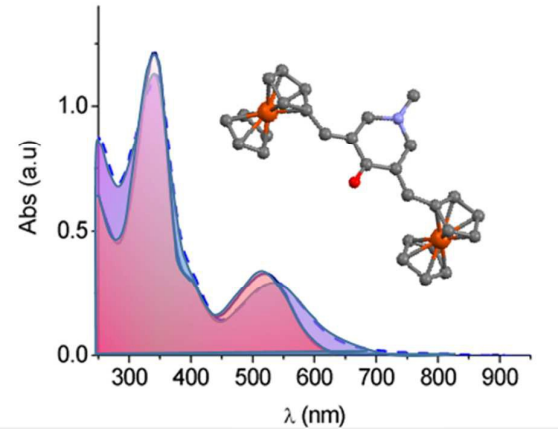

Highlight: Polymorph modifications and conformational isomers were investigated for the title compounds after protonation of the N-atom during chemical and electrochemical experiments.